MINERALOGICAL MAGAZINE, JUNE 1980, VOL. 43, PP. 741-52

Compositional zoning in sodic amphiboles from the blueschist facies

ROBERT MUIR WOOD

Department of Mineralogy and Petrology, Downing Place, Cambridge

SUMMARY. The sodic amphiboles possess two independent chemical substitution series (Fe^{3+}-Al and Fe^{2+}-Mg) that combine to provide a 'plane' of compositions. Yet at no single T and P are compositions covering the whole plane stable: (i) pure riebeckite exists under low-P conditions but breaks down in normal blueschists to give deerite; (ii) ferro-glaucophane is in competition at all except the lowest blueschist temperatures with almandine garnet; (iii) magnesio-riebeckite is stable at high-T and low-P but within the blueschist facies is replaced by the alternative higher density aegirine-talc assemblage; and (iv) glaucophane is stable *only* at high-P.

At higher T and P than those of the blueschists, competition from NaCa pyroxenes, garnets, and deerite first erodes, and then removes, nearly all sodic amphibole compositions. At low-P the normal sodic amphibole-forming reactions from stilpnomelane and chlorite (in the presence of iron oxides, albite, etc.) produce an initial 'riebeckitic' amphibole that subsequently becomes more glaucophanitic with increasing P. Under certain conditions, perhaps connected with hydrous fluid overpressures, these reactions become transposed such that crossitic compositions become replaced whilst ferro-glaucophane to glaucophane compositions remain stable.

THE most important blueschist minerals are the sodic amphiboles with compositions of the form $Na_2M_3^{2+}M_2^{3+}Si_8O_{22}(OH)_2$ in which Fe^{2+} and Mg^{2+} ions compete for the divalent ion site and Fe^{3+} and Al^{3+} for the trivalent; the spread of sodic amphibole compositions can be represented as a square: the Miyashiro diagram. The terminology used throughout this paper is consistent with that proposed by Miyashiro (1957), see fig. 1. Extreme compositions of blueschist-facies rocks that are enriched in M^{2+} and impoverished in M^{3+} may, under certain blueschist-facies conditions, contain tremolite-actinolite or cummingtonite-grunerite amphiboles. Compositional zoning between such amphiboles and the sodic amphiboles is considered in a forthcoming paper.

In order to understand chemical variations amongst the sodic amphiboles the iron concentration measured on the electron probe must be resolved into Fe^{2+} and Fe^{3+} components. This is possible through solving the simultaneous equations for charge balance and site occupancy. In order to demonstrate the superiority of this technique over artificial alternatives (such as that of splitting the iron equally, Ernst, 1979) a partial statistical analysis of the method is presented in Appendix I.

The amphiboles that have formed the substance of this paper were collected from localities in California, Oregon, Washington State, the Alps, and Greece. Further details of specific localities may be found within the following authors' works: Laytonville Quarry exotic block, Mendocino Co., California—Chesterman (1966); Ward Creek, Cazadero, Sonoma Co., California—Coleman and Lee (1963); Panoche Pass, San Benito Co., California—Ernst (1965); Beauregard Creek (South Fork), Santa Clara Co., California and Powers Quarry, Coos Co., Oregon—Muir Wood (1977); Shuksan, Washington State—Brown (1974); Termignon, Haut Savoie, France—Bocquet (1971); Sifnos, Greece—Schliested (1978).

Sodic Amphibole Plane of Compositions

For any blueschist locality, the nearer the sodic amphiboles from all assemblages approach to pure glaucophane, the higher the metamorphic P (Miyashiro and Banno, 1958; Black, 1973; de Roever *et al.*, 1976). Thus riebeckite occurs within the greenschist facies and may even form authigenically (as an isomorphous topotactic replacement product of a brown hornblende: Milton and Eugster, 1959); crossite marks the lowest pressures of blueschist formation (Brown, 1974), and glaucophane is only found at high pressures after the appearance of lawsonite. This simple relationship demonstrates that the pressure stabilization limit is a function of cell volume.

There are many problems in the successful extrapolation to low temperatures of high-T amphibole synthesis because above *c.*500 °C the low-T ordered amphibole species are overtaken by forms with fewer restrictions on site occupancy with: (*a*) variable concentrations of alkali ions on the 'A' site; (*b*) rearrangements of M^{2+} and M^{3+}, with smaller cations invading the large M_4 site; and (*c*) M^{3+} ions moving into the tetrahedral silicon site.

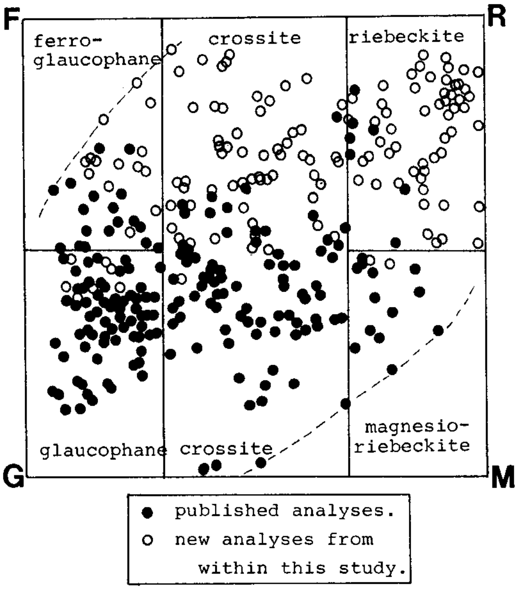

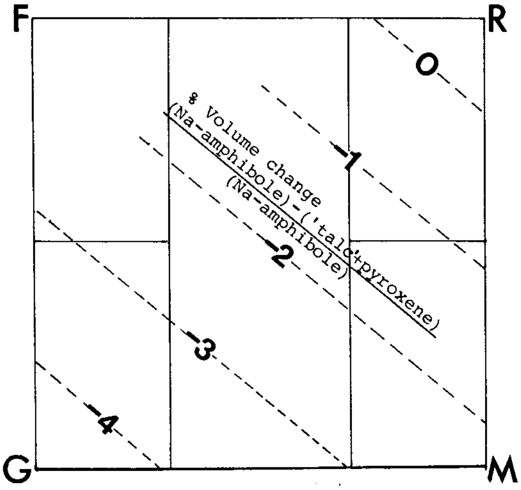

FIGS. 1 and 2. FIG. 1 (*top*). The range of blueschist sodic amphiboles plotted on the Miyashiro diagram. F, R, G, and M stand for the named amphibole end-members, strictly now called pure ferro-glaucophane etc. FIG. 2 (*below*). Relative volume change as a function of composition across the Miyashiro diagram, with regard to the alternative pyroxene-talc mineralogy.

Thus: (1) The 'polymorphic glaucophane transformation' demonstrated by Ernst (1963) was shown by Maresch (1973) to have resulted from a change in chemistry with neither partner in the 'transformation' being glaucophane. Subsequent attempts to synthesize glaucophane have repeated the errors of the earlier results (Maresch, 1977). (2) The magnesio-riebeckite synthesized by Ernst (1960*a*) showed a variation of properties, and hence composition, with regard to the T and fO_2 of synthesis. Which of the amphiboles was magnesio-riebeckite, if any, was not established. (3) The riebeckite synthesized by Ernst (1960*b*) was stable only in the presence of a hematite-magnetite O_2 buffer; at lower fO_2 more Na-rich arfvedsonitic forms were produced. Whilst arfvedsonite is unstable at low-T, natural pure riebeckite is always incompatible with hematite (A. Okay pers. comm.). Accordingly, arfvedsonitic amphibole has grown within the correct fO_2 range for the formation of synthetic riebeckite. (4) Hoffman (1972) formed a ferro-glaucophane through partial reaction between albite–fayalite–quartz in seeded runs at 500 °C (5 kb P_{H_2O}) that decomposed at 350 °C, a temperature at which natural ferro-glaucophanes are stable.

The evidence is therefore clear that at present the stability field of the sodic amphiboles requires interpretation with only cautious experimental analogy.

Mineral inter-relations

(*a*) *Pyroxenes.* Compositions are now known that cover approximately the whole of the sodic amphibole plane, and there is no evidence of any internal immiscibility (fig. 1). At no single P and T, however, are all compositions across the system stable.

The simplest alternative mineralogy is that of the isochemical assemblage of Na pyroxene + talc mineral; or alternatively albite + talc mineral with additional quartz. Thus:

(1) $Mg_6Si_8O_{20}(OH)_4 + 4NaAlSi_2O_6 = 2Na_2Mg_3Al_2Si_8O_{22}(OH)_2$

(2) $Mg_6Si_8O_{20}(OH)_4 + 4NaFe^{3+}Si_2O_6 = 2Na_2Mg_3Fe^{3+}_2Si_8O_{22}(OH)_2$

(3) $Fe^{2+}_6Si_8O_{20}(OH)_4 + 4NaAlSi_2O_6 = 2Na_2Fe^{2+}_3Al_2Si_8O_{22}(OH)_2$

(4) $Fe^{2+}_6Si_8O_{20}(OH)_4 + 4NaFe^{3+}_2Si_2O_6 = 2Na_2Fe^{2+}_3Fe^{3+}_2Si_8O_{22}(OH)_2$

(5) $4NaAlSi_3O_8 + Mg_6Si_8O_{20}(OH)_4 = 2Na_2Mg_3Al_2Si_8O_{22}(OH)_2 + 4SiO_2$

(6) $4NaAlSi_3O_8 + Fe^{2+}_6Si_8O_{20}(OH)_4 = 2Na_2Fe^{2+}_3Al_2Si_8O_{22}(OH)_2 + 4SiO_2$

From the volume changes for these reactions calculated at 25 °C, 1 bar (data from Helgeson *et al.*, 1978), and with the assumption of complete and ideal solid solution between the end-member pyroxenes and talc minerals (see below), it is possible to calculate dV/dX for the whole sodic amphibole plane (fig. 2). For all compositions except those close to the riebeckite end-member, the pyroxene + talc assemblage is of higher density than the associated amphibole.

Only the binary glaucophane-magnesioriebeckite system is realistically described by this simple model. The calculated dP/dT of reaction (1) is 12.77 bars per °C (data from Helgeson *et al.*, 1978); its position for 'true' glaucophane will be closer to that of the albite breakdown reaction than that discovered for 'pseudo' glaucophane by Carman (1974).

The low-P synthetic reaction products of glaucophane include a 'sodic-montmorillonite-type-mineral', whilst the low-P and low-T reactions forming natural glaucophane are between albite and serpentine, or talc. The relative compatibilities of the glaucophane-forming minerals are plotted in the NaAl–Si–Mg ternary system in fig. 3, and the approximate reaction grid for glaucophane-formation is constructed in fig. 4. In parallel with the phase relations of jadeite, glaucophane may form at lower P in the absence of quartz.

The aegirine-jadeite system is highly asymmetrical; the range of aegirine solid solution towards jadeite increases only slowly with pressure (Popp and Gilbert, 1972). Thus compositions with more than 80% magnesio-riebeckite are unstable in the blueschist facies (fig. 5). Pure magnesio-riebeckites are restricted to higher T, lower P metamorphics, particularly crocidolite asbestos deposits; the limit of solid solution being dependent on high T/P.

The actual competition between pyroxenes and the full range of sodic amphiboles is complicated by the additional possibilities of solid solution towards augite. In parallel with the position of riebeckite *vis-à-vis* sodic amphiboles, aegirine is the only pyroxene stable under low-P, low-T hydrous conditions. The augitic solid solution that in blueschists rarely extends beyond Na/Ca of 1/1 tends towards the sodic amphibole M^{2+}/M^{3+} ratios. Thus pyroxene can only form from amphibole through: (1) oxidation; (2) reaction with an earlier Fe^{3+}-rich mineral such as aegirine, or an aluminous mineral such as lawsonite, epidote, or phengite; or (3) through the production of another higher $(Fe^{2+} + Mg)/(Fe^{3+} + Al)$ mineral. All such reactions, even those involving epidote or lawsonite, require additional Ca, some of which may be provided through the lowering of the garnet-grossular content in passing from blueschist to

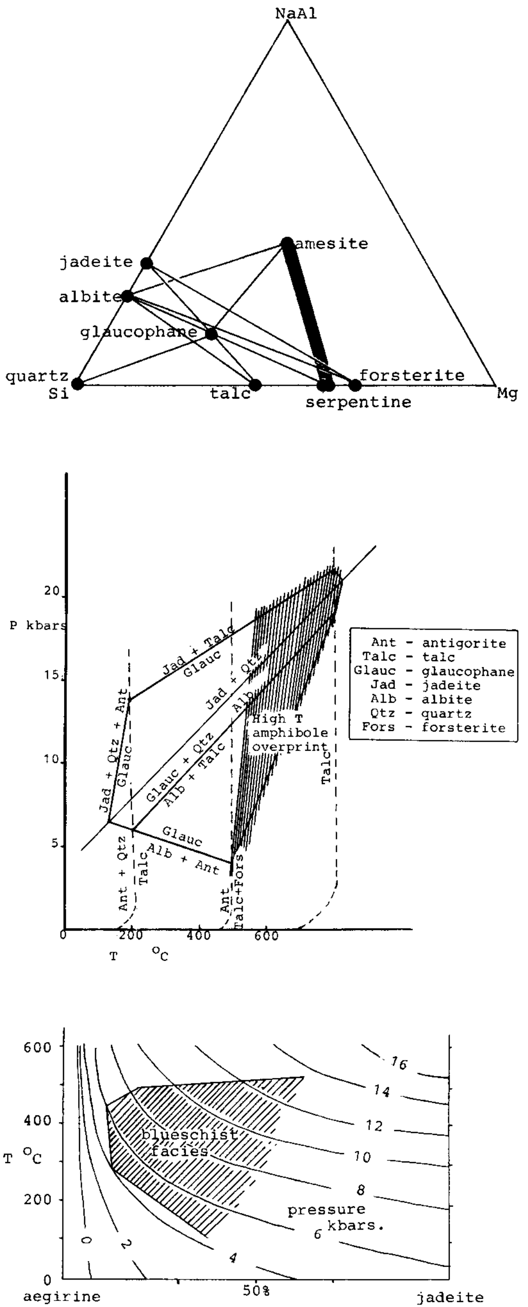

FIGS. 3–5. FIG. 3 (*top*). Glaucophane within the Mg–NaAl–Si ternary system. FIG. 4 (*middle*). The P–T reaction grid for glaucophane formation. FIG. 5 (*below*). The solid solution limits of the glaucophane-magnesio-riebeckite amphiboles due to competition from the pyroxene-talc assemblage: jadeite–aegirine solid solution vs. T, with isobaric contours.

eclogite. If pyroxenes are restricted through lack of available Ca to more sodic compositions, sodic amphiboles can survive into higher *P* and *T* conditions.

The back-reaction from a blueschist eclogite (as found in Sifnos assemblages) is written as reaction (7).

(7) $15NaCaFe^{2+}_{0.5}Mg_{0.5}Al_{0.5}Fe^{3+}_{0.5}Si_4O_{12} + 3Fe^{2+}_2Mg_{0.5}Ca_{0.5}Al_2Si_3O_{12} + 8.5H_2O = 2Ca_2Al_{2.4}Fe^{3+}_{0.6}Si_3O_{12}(OH) + 7.5Na_2Fe^{2+}_{1.8}Mg_{1.2}Fe^{3+}_{0.84}Al_{1.16}Si_8O_{22}(OH)_2 + 12.5CaO$

Sodic amphibole has also formed at Sifnos through the back-reaction between pyroxene and deerite: reaction (8).

(8) $6NaCaFe^{2+}_{0.5}Mg_{0.5}Al_{0.5}Fe^{3+}_{0.5}Si_4O_{12} + Fe^{2+}_{12}Fe^{3+}_6Si_{12}O_{40}(OH)_{10} + H_2O + 3Na_2O = 6Na_2Fe^{2+}_{2.5}Mg_{0.5}Al_{0.5}Fe^{3+}_{1.5}Si_8O_{22}(OH)_2 + 6CaO$

The lower grade back-reaction from aegirine-augite to aegirine and riebeckite (found in Cazadero meta-ironstones) is written as reaction (9).

(9) $3NaCaFe^{2+}_{0.67}Mg_{0.33}Al_{0.17}Fe^{3+}_{0.83}Si_4O_{12} + H_2O = NaFe^{3+}Si_2O_6 + Na_2Fe^{2+}_2Mg_1Al_{0.5}Fe^{3+}_{1.5}Si_8O_{22}(OH)_2 + 2SiO_2 + 3CaO$

As the pyroxenes possess a dimension of solid solution beyond that of the sodic amphiboles, the plexus of compatibilities becomes correspondingly more difficult to disentangle. To demonstrate how the ideal reactions relate to real pyroxene-amphibole compatibilities, fig. 6, a Fe^{2+} vs. Fe^{3+} grid has been constructed.

Although the mineral omphacite is known to interrupt the intervening jadeite-diopside solvus, its variety of structural states (Carpenter, 1979) compounds the problems of its experimental reproduction and prevents its simple use as a *P-T* indicator. The extension of such Fe-free, NaCa-pyroxenes towards aegirine, extends the NaCa-pyroxene stability field to lower *P*. As can be seen in fig. 6, the chemical competition from the pyroxenes, as might be predicted, extends out from the magnesio-riebeckite 'corner'.

(*b*) *Stilpnomelane-chlorite*. For sodic amphiboles with moderate to high Fe^{2+} enrichment the hypo-

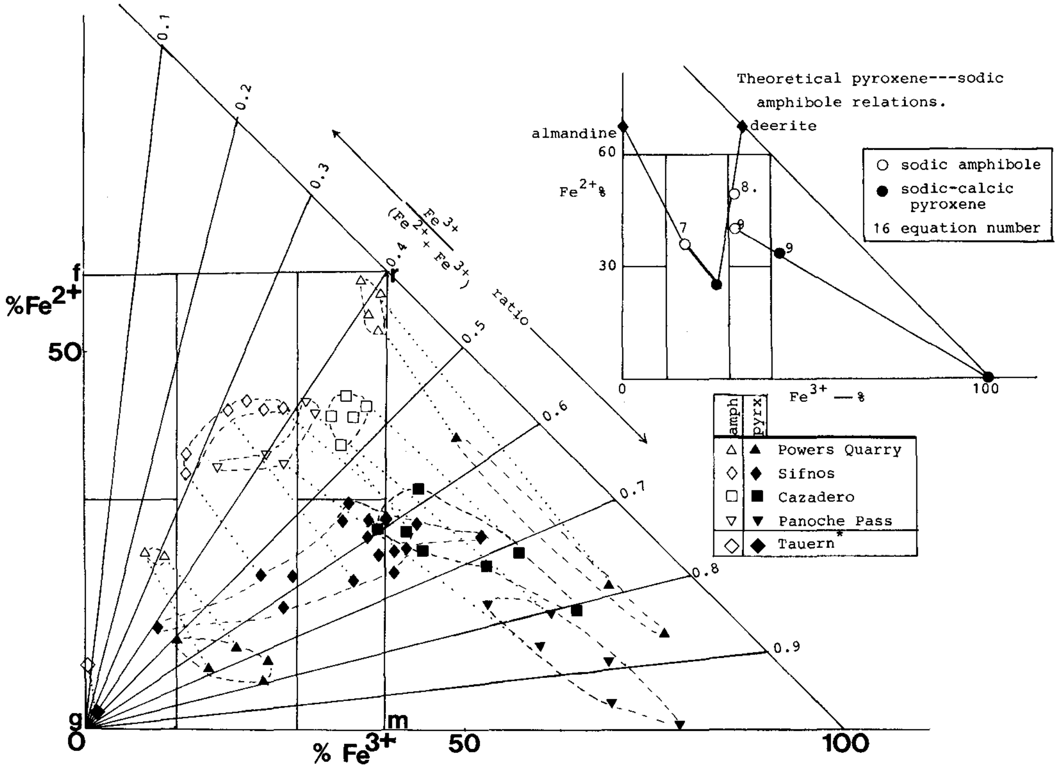

FIG. 6. Sodic amphibole-pyroxene inter-relations on the Fe^{2+} vs. Fe^{3+} system.

thetical alternative pyroxene + talc-mineral assemblage is complicated, first, by the problematic nature of the solid solution between talc and minnesotaite (there is no proof of isostructurality), and secondly by the presence of two rival low grade sheet silicate minerals: stilpnomelane and chlorite. Although both these minerals have a considerable potential for solid solution their blueschist-greenschist chemistry is remarkably univariant. Chlorites contain 30–34 % Al/(Al + Fe + Mg), with higher values for more Mg-rich forms, whilst the Fe/(Al + Fe + Mg) ranges from 25–60 %. The stilpnomelanes contain 15–20 % Al/(Al + Fe + Mg) and 40–80 % Fe/(Al + Fe + Mg), though some localities show a gap in the compositional spread for the middle range of iron concentrations. Although low-P stilpnomelanes are predominantly Fe^{2+}-rich, there is evidence (presented below) that ferri-stilpnomelanes are stable blueschist minerals.

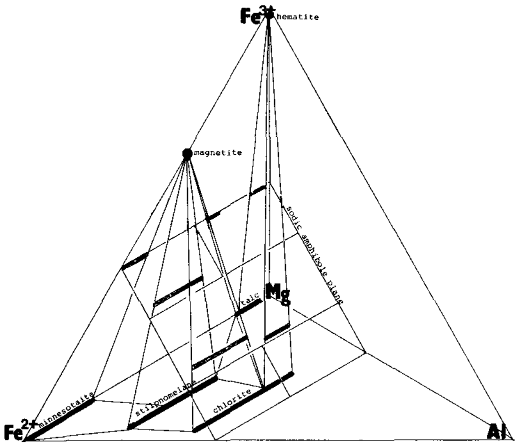

FIG. 7. The interception of low-grade mineral compatibilities by the sodic amphibole plane; the Fe^{2+}–Mg–Al–Fe^{3+} quaternary system.

The pre-blueschist phase relations for these Fe^{2+}- and Al-rich assemblages can be plotted within the Mg-Al-Fe^{2+}-Fe^{3+} system (fig. 7). The low-P, low-T sodic amphibole-formation reactions involve the minerals chlorite, minnesotaite, stilpnomelane, magnetite, and quartz with, for more magnesian compositions, talc and hematite.

All crossite-riebeckite-formation reactions require excess Na beyond that which can be supplied by earlier albite, as the Na/Al ratio of sodic amphiboles is $\geqslant 1$. In ferruginous assemblages, and even in some metabasites (A. Okay, pers. comm.), aegirine may be present within the pre-blueschist assemblage from an earlier episode of Na-infiltration. The reaction of aegirine + chlorite to sodic amphibole is delayed to higher P than that in which there was no pre-existing pyroxene, though once the amphibole is stable pyroxene-chlorite become incompatible. As albite is the only significant low-grade sodic mineral, Na is liberated through the degradation of albite (or plagioclase) to a mineral, or minerals, in which $Na/Al < 1$. The limited availability of Na restricts the first-formed sodic amphibole to higher P and to compositions where Na/Al is closer to unity.

For lower Fe^{2+}/Mg rock compositions stilpnomelane is missing from the low grade assemblage and chlorite extends its compatibility uninterrupted over to the riebeckite-magnesioriebeckite boundary. Hence ideally the first-formed amphibole within Mg-rich, low grade blueschist pelites and basites lies towards this boundary whilst for Mg-poor pelites the amphibole forms at the stilpnomelane-magnetite conjunction with the sodic amphibole plane (fig. 7). Whilst all these first-formed amphiboles appear to have Fe^{2+}/Mg [sodic amphibole] = Fe^{2+}/Mg [chlorite] = Fe^{2+}/Mg [rock], until more glaucophanitic compositions become stabilized with pressure the Fe^{3+}/Al content of the amphibole remains in advance of that of the rock.

The reaction between Fe-rich chlorite with magnetite and quartz to form a riebeckitic sodic amphibole generates an additional aluminous mineral; perhaps phengite (if excess K) or lawsonite (if excess Ca). On increasing pressure the first-formed Fe^{3+}-rich sodic amphibole reacts with albite and additional chlorite to form an aluminous sodic amphibole: as in 'A' and 'B' in fig. 8. The reaction between stilpnomelane and magnetite (with quartz) can generate a sodic amphibole without any surplus Al; through the additional higher P reaction between albite and stilpnomelane this alters to ferro-glaucophane, as 'C' in fig. 8.

Some good examples of growth-zoned amphiboles come from Laytonville Quarry quartzites. Crossites form rhombohedral prism-shaped crystals up to 10 mm in length that are visibly zoned from darker blue cores to pale blue rims: the chemical zoning profile of one of these is presented in fig. 9. They have grown within a quartzite distorting a schistose texture of phengites and compositional banding of varying concentrations of tiny garnets. In most assemblages the riebeckite-crossite cores of the amphiboles have been partially or totally replaced by stilpnomelane and quartz, whilst the almost homogeneous ferro-glaucophane rims remain intact. Out of about twenty crossite quartzites collected from the quarry only one rock (109780) contained a variation on the standard reaction texture with smaller crossites that were neither

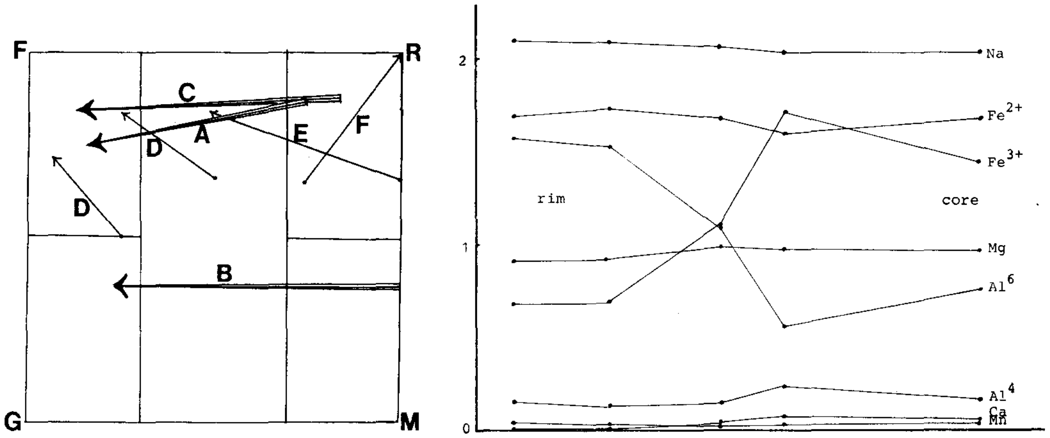

FIGS. 8 and 9. FIG. 8 (*left*). Ideal sodic amphibole reactions plotted on the Miyashiro diagram, labelled as in fig. 1. FIG. 9 (*right*). Crossite zoning profile from C55 Laytonville Quarry.

zoned nor atolled, but instead had undergone resorption via crystal fragmentation along the cleavage traces. Some crossite textures are illustrated in fig. 10.

One rock (102497) has crossite cores entirely replaced by fine grained chlorite and quartz, that is itself, in some areas, undergoing partial reaction to stilpnomelane. Within some of the remaining crossite cores there are fragments of exsolved Fe-oxide lying parallel with the amphibole *c* axis. These crossite cores have higher Mg and lower Fe^{3+} than those from other assemblages.

In many rocks large sheaves of late-stage stilpnomelane cut across all the earlier textures and take their components from the cores of neighbouring crossites that are themselves replaced by quartz. Whilst these 'external' stilpnomelanes are sometimes Fe^{2+}-rich the 'internal' crossite-replacing stilpnomelanes are nearly all partially oxidized forms.

The simple explanation for the development of atoll texture has been outlined in Muir Wood (1979*b*). The atolled mineral was originally zoned during progressive metamorphic growth; subsequent hydration stabilized stilpnomelane that competes for the material of the first-formed amphibole core; as in reaction 10.

$$(10)\quad 2.8Na_2Fe^{3+}_{1.29}Al_{0.71}Fe^{2+}_{2.1}Mg_{0.9}Si_8O_{22}(OH)_2 + 5.2H_2O + K_2O$$
$$= 2.8Na_2O + K_2Fe^{3+}_{3.61}Fe^{2+}_{5.88}Mg_{2.52}Si_{16}Al_2(O_{40}OH_{16}) + 6.4SiO_2$$

On the plot of Fe–Mg–Al of fig. 11, the replacing stilpnomelane has an identical Fe:Mg:Al value to that of the crossite core only when the stilpnomelane can incorporate all the Fe^{3+} as well as the Fe^{2+}; thus demonstrating that the stilpnomelane formed partly oxidized. The chlorite from the 102497 amphibole cores is, however, only equivalent to the crossite composition when its Fe^{3+} content is neglected; it is this excess Fe^{3+} that forms the exsolved Fe oxide lamellae. A back-reaction between the chlorite and the Fe oxide (plus K) can itself generate stilpnomelane.

From several assemblages, some of the more aluminous crossite centres are only partly resorbed, leaving tiny slivers of ferro-glaucophane embedded in the replacing quartz (fig. 10, sketch 5).

Although chlorite is replacing some of the more magnesian crossite cores, chlorite cannot be the stable equivalent of the sodic amphiboles or the ferro-glaucophane rims would not be left intact (decomposition would follow the reverse of 'A' in fig. 8); and yet the full range of stilpnomelane compositions are stable, This contrasts with the amphibole growth-zoning that resulted from the 'prograde' breakdown of stilpnomelane *before* chlorite. Thus the relative inter-relationships of chlorite and stilpnomelane have become transposed, making crossite unstable whilst ferro-glaucophane remains stable (fig. 12).

The late-stage hydration episode can be traced through many of the Laytonville Quarry assemblages; the mineralogy that appeared at this period includes: riebeckite, stilpnomelane, actinolite, howieite, minnesotaite, ekmanite, pumpellyite, and chlorite; minerals that are all stable at the low-*T* greenschist-blueschist boundary. Although there was no shortage of K within these crossite-phengite quartzites necessary for stilpnomelane formation, the chlorite may in some instances have marked an

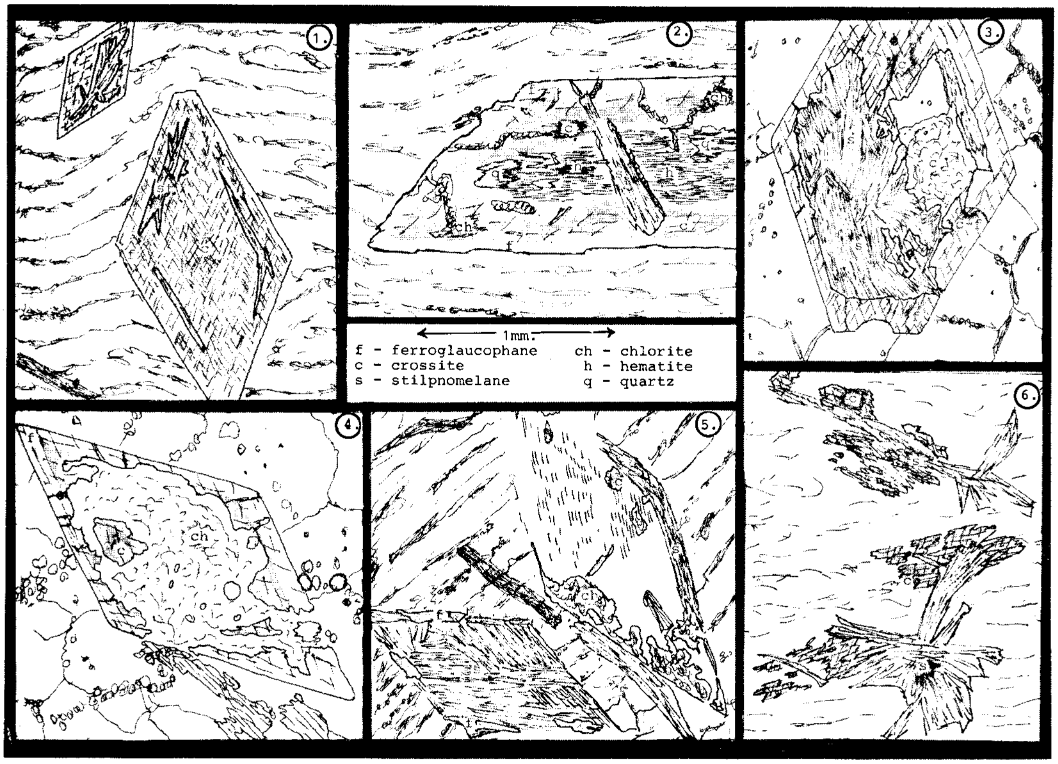

FIG. 10. Crossite resorption textures from Laytonville Quarry: 1. 102506, 2. 102495, 3. PA6, 4. 102497, 5. PA18, 6. 109780.

intermediate reaction-step caused by local and temporary K-deficiency.

In Powers Quarry assemblages, reactions may be followed that are the reverse of those from Laytonville Quarry: stilpnomelane schists contain secondary ferro-glaucophanes, glaucophanes, and a few riebeckites, but no crossites (fig. 13). Such a configuration of stable sodic amphiboles is very dependent on a_{K^+}. Low a_{K^+} in the Panoche Pass metamorphic rocks restricts stilpnomelane to a rare late stage vein-accessory mineral. Of all the localities studied, this is the only one in which amphiboles zone from glaucophane- and crossite-rich cores to riebeckite rims, right through the region 'normally' interrupted by stilpnomelane (fig. 14).

(*c*) *Deerite-garnet.* At higher *P* and *T* deerite and garnet compete with the Fe^{2+}-rich sodic amphiboles. A simple reaction may be written between pure ferro-glaucophane and almandine (11).

$$(11)\quad Na_2Fe_3^{2+}Al_2Si_8O_{22}(OH)_2 = Fe_3^{2+}Al_2Si_3O_{12} + 5SiO_2 + H_2O + Na_2O$$

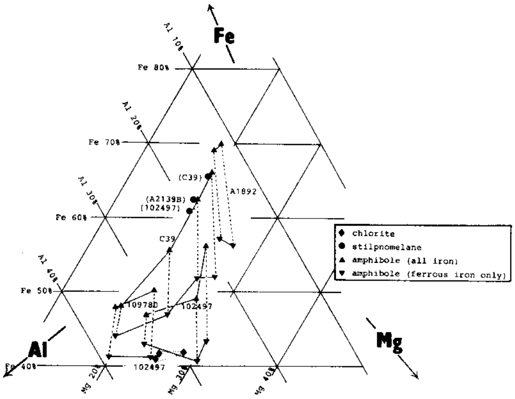

FIG. 11. Laytonville Quarry zoned crossites and their replacement mineralogy plotted on the Fe-Mg-Al ternary system.

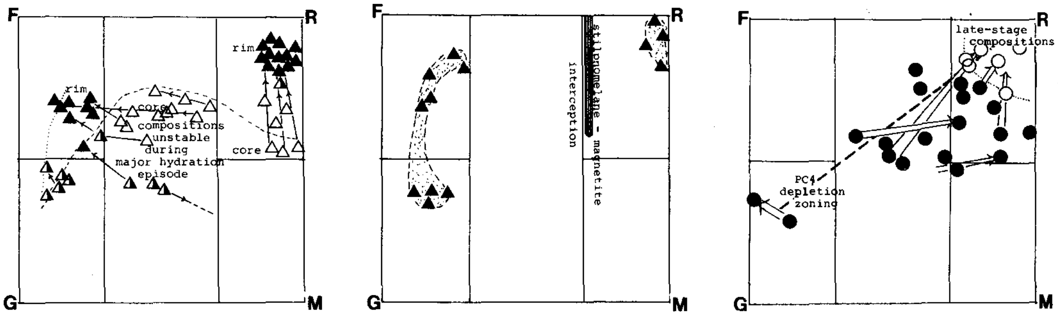

FIGS. 12-14. FIG. 12 (*left*). Laytonville Quarry sodic amphiboles: the Miyashiro diagram. FIG. 13 (*centre*). Powers Quarry sodic amphiboles: the Miyashiro diagram. FIG. 14 (*right*). Panoche Pass sodic amphiboles: the Miyashiro diagram.

Natural ferro-glaucophanes never approach closer than about 80 mol % pure ferro-glaucophane, as a result of competition from the garnet; see fig. 15, the Na–Fe^{2+}–Al–Si quaternary system. Garnet formation during progressive metamorphism is dependent on local Mn concentrations. For natural rock compositions, under natural fluid activities (particularly a_{Na^+}) pure ferro-glaucophane becomes overtaken by the formation of spessartine–almandine garnet, yet in Fe^{2+}-rich, Mn-free pelitic schists at high-*P* and very low-*T*, pure ferro-glaucophane should be stable. Minor ionic contamination from Fe^{3+} and Mg ensures that compositions so far discovered remain offset.

With increase of *T* there is an exchange of components such that as the garnet progressively enriches in almandine, the amphibole retreats away from ferro-glaucophane. Reaction lines 'D' and 'E' on fig. 8 demonstrate the change in amphibole compatibilities occasioned on decreasing grade ('D' is from 1:2 to 2:1 spess:alm; 'E' is from 1:1:4 to 2:0:1 spess:pyr:alm). On fig. 16 the ferro-glaucophane–garnet reactions are plotted on a_{Na^+} vs. a_{OH^-}. As demonstrated in this system, the presence of Mn not only raises the water activity at which garnet is stable but also restricts compatible ferro-glaucophane to higher a_{Na^+}.

The lower *T* stability for almandine (500 °C) and spessartine (400 °C) (Hsü, 1968) are certainly overestimates: as one of many examples, spessartines occur in Powers Quarry assemblages that have not exceeded 300 °C.

Sodic amphibole compositions that coexist with almandine-pyrope garnets are (with excess SiO_2, Na^+, and OH^-) restricted to a univariant line for a given *P* and *T*. As natural blueschist garnets are also enriched in grossular and spessartine, the relative partitioning between amphibole and garnet depends on the almandine/ferro-glaucophane and

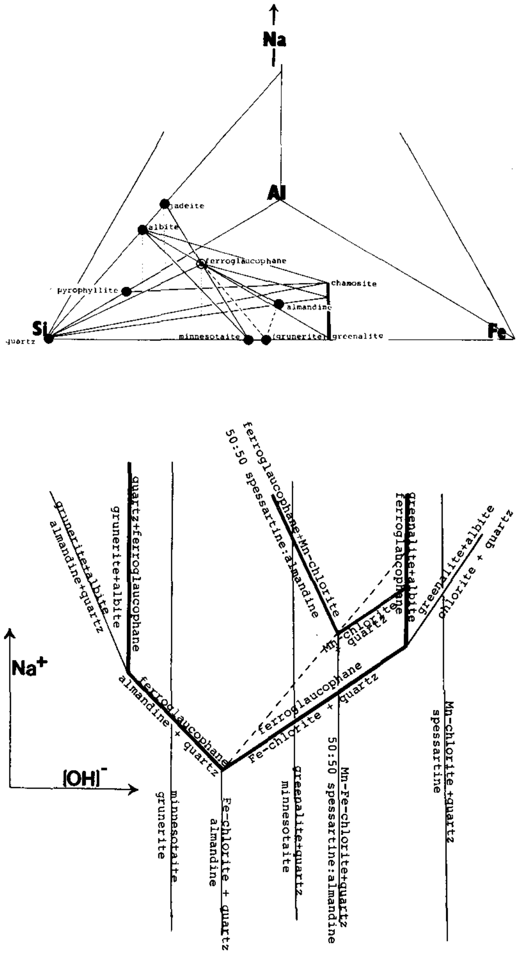

FIGS. 15 and 16. FIG. 15 (*top*). Ferro-glaucophane within the Fe^{2+}–Na–Al–Si system. FIG. 16 (*below*). Sodic amphibole garnet stabilities: a_{Na} vs. a_{OH}.

pyrope/glaucophane 'components' within the solid solution. Thus with excess SiO_2, Na^+, and $(OH)^-$:

$$\frac{Fe_3^{2+}Al_2\ (\text{garnet})}{Fe_3^{2+}Al_2\ (\text{amphibole})} = k_{1(P,\,T)} \text{ and } \frac{Mg_3Al_2\ (\text{garnet})}{Mg_3Al_2\ (\text{amphibole})} = k_{2(P,\,T)}$$

$k_2 \ll 1$, at normal blueschist pressures but increases towards blueschist-eclogite conditions. Garnet-amphibole partitioning behaviour has been plotted on fig. 17. It can be seen that: (*a*) the more complex Franciscan localities contain two limits of partitioning that correspond to a range of metamorphic conditions; high k_1 values represent peak T (and P), low k_1 values mark the limit of the secondary blueschist hydrations; (*b*) that at high 'grades' spessartine-grossular garnets only coexist with grunerite. With both k_1 and k_2 considered as ideally unrelated to composition ($k_1 = 1.5$; $k_2 = 0.0166$) and as mutually independent, coexisting garnet compositions have been plotted on the Miyashiro diagram in fig. 18. On decreasing P or T the fixed garnet compositions coexist with amphiboles closer to ferro-glaucophane. Garnet resorption adjacent to homogeneous rims on Laytonville Quarry zoned crossites indicates that such amphibole grew at the expense of almandine during an earlier hydration episode.

The second 'high-grade' blueschist mineral that interferes with the spread of sodic amphiboles is deerite. Under normal blueschist conditions riebeckite breaks down to the denser deerite-quartz-magnetite assemblage liberating Na^+. A high a_{Na^+} may preserve riebeckite to higher P just as low a_{Na^+} will encourage its lower P breakdown. Under a high P_{H_2O} and moderate a_{Na^+} magnetite and quartz react to form deerite and aegirine. From the evidence of certain blueschist facies ironstones (from Termignon and Panoche Pass), riebeckite breakdown normally precedes the reaction between magnetite and quartz probably because the former reaction is less dependent on a low a_{Na^+}. The various reactions connecting deerite and riebeckite have been plotted as a function of a_{Na^+} and a_{OH^-} in Muir Wood (1979*c*).

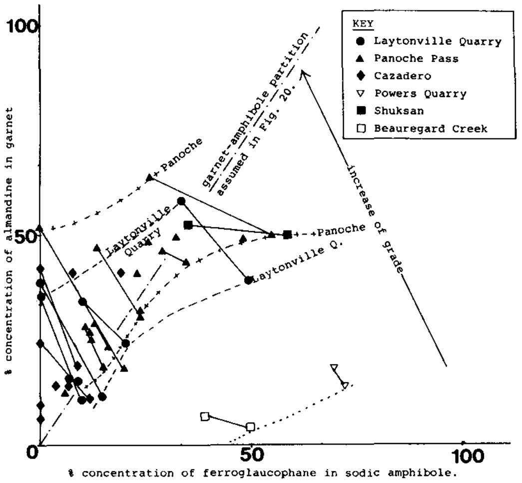

FIG. 17. Relative partitioning between almandine content of garnet and ferro-glaucophane content of sodic amphibole.

Within Laytonville Quarry and Cazadero meta-ironstones the early amphiboles that coexisted with deerite lie towards magnesio-riebeckite. At both localities late-stage hydration has caused the partial breakdown of deerite to form an alternative low grade pure riebeckite and stilpnomelane compatibility; reaction (12) and 'F' in fig. 8.

$$\begin{aligned}(12)\quad & K_2Mg_4Fe_8^{2+}Si_{16}Al_2(O_{40}OH_{16})+\\ & 12Na_2Fe_2^{3+}Fe_3^{2+}Si_8O_{22}(OH)_2\\ & = 3Fe_{12}^{2+}Fe_6^{3+}Si_{12}O_{40}(OH)_{10}+\\ & 4Na_2Fe_2^{2+}MgFe_{1.5}^{3+}Al_{0.5}Si_8O_{22}(OH)_2+\\ & 44SiO_2+8Na_2O+K_2O+H_2O\end{aligned}$$

The range of amphiboles that can coexist with deerite is determined by the grade of metamorphism and the Mn concentration. In the Mn-poor ferruginous assemblages of the Alps, the crossites coexisting with deerite are more $Al+Fe^{2+}$-rich than those from the Franciscan. On increasing grade such crossites would react with a spessartine-rich garnet (under typical Alpine metamorphic conditions almandine is incompatible with deerite) to liberate sodium and to form the amphibole-garnet-deerite assemblage that is typical of the Franciscan; reaction (13).

$$\begin{aligned}(13)\quad & Mn_2Fe^{2+}Al_sSi_3O_{12}+\\ & 2Na_2Fe^{3+}AlMg_{0.5}Fe_{2.5}^{2+}Si_8O_{22}(OH)_2+\\ & 0.5Fe_{11}^{2+}MnFe_6^{3+}Si_{12}O_{40}(OH)_{10}\ (\text{Alpine})\\ & = 2Mn_{0.5}Fe_{2.5}^{2+}Al_2Si_3O_{12}+\\ & Na_2Fe_2^{3+}MgFe_2^{2+}Si_8O_{22}(OH)_2+\\ & 0.5Fe_{10}^{2+}Mn_2Fe_6^{3+}Si_{12}O_{40}(OH)_{10}+\\ & H_2O+Na_2O+5SiO_2\end{aligned}$$

At the highest grades of blueschist metamorphism, at the boundary with blueschist eclogites, deerite, garnet, and omphacite-chloromelanite may take the place of most compositions across the sodic amphibole plane, leaving only amphiboles close to glaucophane stable.

Oxidation indicators

The freedom for Fe^{2+} and Fe^{3+} solid solution offered by the sodic amphiboles makes them potentially sensitive indicators of the local oxidation state that is itself, through its distribution within the

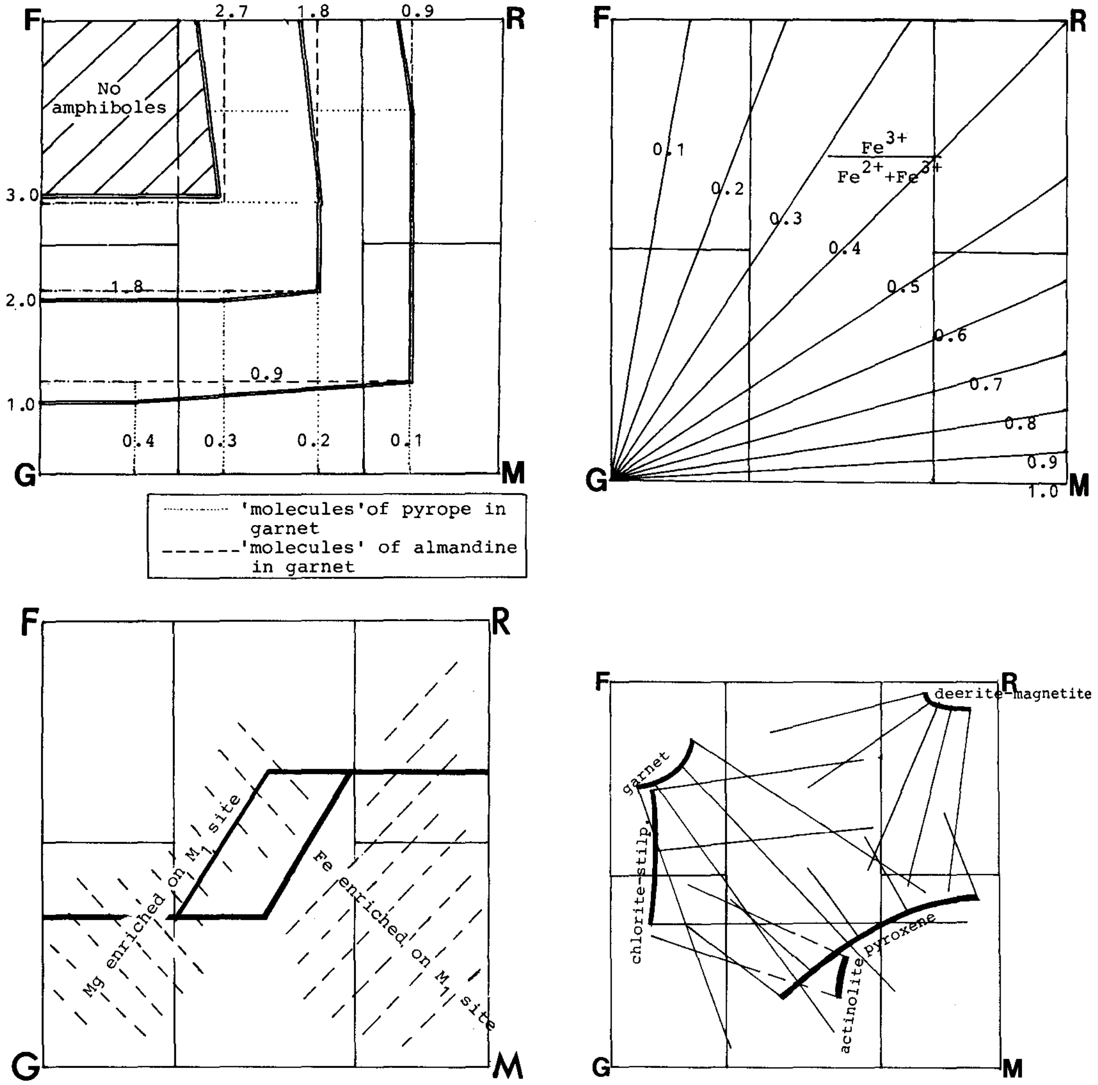

FIGS. 18–21. FIG. 18 (*top left*). Ideal garnet-amphibole partitioning behaviour: the Miyashiro diagram. FIG. 19 (*top right*). Ideal oxidation ratio across the Miyashiro diagram. FIG. 20 (*lower left*). Variations in divalent ion site-occupancy across the Miyashiro diagram. FIG. 21 (*lower right*). Ideal mineral-consuming zoning vectors across the Miyashiro diagram.

minerals, controlling the local fO_2. If the mineral/bulk-rock composition partition coefficients are unity then the oxidation ratio of the rock relates to the amphibole composition as in fig. 19. Yet the effect of the progressive enrichment of glaucophane during increase of pressure is to produce a single amphibole composition at the limit of the sodic amphibole field for a range of oxidation states. Only when the whole range of sodic amphiboles are stable can amphibole composition be an oxidation indicator. Thus although Brown (1974) discovered in Shuksan assemblages that the hematite-magnetite oxygen buffer coexisted with a range of amphibole compositions of roughly constant Fe^{2+}/Mg ratio, these amphiboles also coexisted with chlorite and, or, stilpnomelane and quartz, equilibrium compatibilities that are impossible without a Na^+ deficiency. The rocks on close study reveal sequential assemblages and amphibole zoning.

Variations in site occupancy for Fe^{2+} and Mg^{2+} on the M_1 and M_3 sites, discovered through Mossbauer spectroscopy (Bancroft and Burns, 1969;

Ernst and Wai, 1970) suggest that the change of ion-site occupancies across the sodic amphibole plane involves Mg-enriched M_1 site for glaucophanes and Fe^{2+}-enriched M_1 site for the riebeckites (fig. 20) that would bend the ideal oxidation variation lines of fig. 19 to more nearly parallel Fe^{2+}/Mg contours.

Conclusions

A summary of zoning paths resultant on shifting amphibole-coexisting mineral compatibilities is presented in fig. 21. A specific vector of growth zoning will on reversal of conditions provide a specific opposed vector of resorption. Only progressive metamorphic growth zoning seems to be of great importance for the amphiboles as both Fe^{3+}/Al and Fe^{2+}/Mg ratios approximate to those of the bulk chemistry and minor elements do not substitute preferentially. Because mineral growth at low grades tends to be restricted to periods of enhanced ionic mobility that accompany deformation episodes and hydrous infusion, true progressive metamorphic zoning is unusual, and for these sodic amphiboles, is dependent on a high initial a_{Na^+}.

Many of the amphiboles that have formed in high-grade eclogite-blueschists are from secondary hydration episodes which have been transient and therefore at constant P–T. As a result many late-stage amphiboles form homogeneous grains, although where there was a pre-existing amphibole, core-rim zoning may form as a result of overgrowth and inter-reaction that may appear to be 'progressive', instead of from discrete reaction episodes.

As low-T sodic amphiboles cannot be synthesized it is impossible to quantify directly the relative partition coefficients although one alternative might be to study assemblages in which the amphibole coexists with two other minerals for which the mutual partition coefficients are already known. Råheim and Green (1974) calibrated the garnet-pyroxene Fe^{2+}/Mg partition and extrapolated high-T results to those of the blueschists, making certain assumptions about the ideality of the low-T jadeite-diopside system that are inconsistent with subsequent discoveries about the nature of site degeneracy in omphacites (Carpenter, 1979). Although such data provide the only useful framework on which mutual sodic amphibole partitions may be located, there are many problems. Thus in pyroxenes and garnets the Fe^{2+} and Mg^{2+} ions occupy single structural sites whilst in the sodic amphiboles they are found on two positions (M_1 and M_3) that alter their Mg/Fe^{2+} partitioning according to the over-all Al/Fe^{3+} ratio (Bancroft and Burns, 1969; Ernst and Wai, 1970). Also, pyroxene-garnet-sodic-amphibole assemblages have usually arisen through secondary hydration of an eclogite. In some specific instances (Holland, 1979) there may be sufficient evidence to consider the coexisting minerals as compatible, but in general, as only compositions at the extreme outer margins of the zoned higher grade mineralogy can be used, much partition coefficient information is likely to be erroneous.

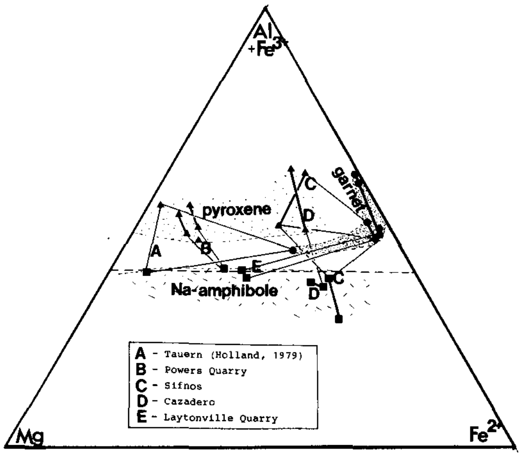

FIG. 22. Garnet-pyroxene-amphibole compatibilities in the Mg–Fe^{2+}–$(AlFe^{3+})$ ternary system.

Some garnet-pyroxene-amphibole compatibilities are plotted in fig. 22. Amphibole Fe^{2+}/Mg lies between pyroxene Fe^{2+}/Mg and garnet Fe^{2+}/Mg though much closer to the former; typical amphibole/pyroxene values are around 2. As in many blueschist garnets, Mg is a trace element, a full tripartite coefficient map is at present unrealizable.

REFERENCES

Bancroft (G. M.) and Burns (R. G.), 1969. *Mineral. Soc. Am. Special Paper*, **2**, 137.

Black (P. M.), 1973. *Contrib. Mineral. Petrol.* **39**, 55.

Bocquet (J.), 1971. *Eclog. Geol. Helv.* **64**, 71.

Brown (E. H.), 1974. *Bull. geol. Soc. Am.* **85**, 333.

Carman (J. H.), 1974. *Am. Geophys. Union Trans.* **55**, 481.

Carpenter (M. A.), 1979. *Am. Mineral.* **64**, 102.

Chesterman (C. W.), 1966. *Calif. Div. Mines and Geol. Bull.* **190**, 503.

Coleman (R. G.) and Lee (D. E.), 1963. *J. Petrol.* **4**, 260.

de Roever (E. W. F.), Beunk (F. F.), and Kieft (C.), 1976. *Contrib. Mineral. Petrol.* **58**, 221.

Ernst (W. G.), 1960*a*. *Geochim. Cosmochim. Acta*, **19**, 10.

—— 1960*b*. *J. Geol.* **70**, 689.

—— 1963. *Am. Mineral.* **48**, 241.

—— 1965. *Bull. geol. Soc. Am.* **76**, 879.

—— and Wai (C. M.), 1970. *Am. Mineral.* **55**, 1226.

—— 1979. *Mineral. Mag.* **43**, 269.

Eskola (P.), 1929. *Geol. Fören. Stockholm Förh.* **51**, 157.

Helgeson (H. C.), Delany (J. M.), Nesbitt (H. W.), and Bird (D. K.), 1978. *Am. J. Sci.* **278A,** 1.
Hoffman (C.), 1972. *Contrib. Mineral. Petrol.* **34,** 135.
Holland (T. J. B.), 1979. *J. Geol.* **87,** 1.
Hsü (L. C.), 1968. *J. Petrol.* **9,** 40.
Maresch (W. V.), 1973. *Earth and Planet. Sci. Lett.* **20,** 385.
—— 1977. *Tectonophysics,* **43,** 109.
Milton (C.) and Eugster (H. P.), 1959. In *Researches in Geochemistry,* (ed. P. H. Abelson), p. 118. J. Wiley, New York.
Miyashiro (A.), 1957. *J. Fac. Sci. Univ. of Tokyo,* II, **11,** 57.
—— and Banno (S.), 1958. *Am. J. Sc.* **256,** 97.
Muir Wood (R.), 1977. *Ph.D. Thesis,* Cambridge.
—— 1979*a*. *Geol. Mag.* **116,** 21.
—— 1979*b*. Ibid., 191.
—— 1979*c*. *Mineral. Mag.* **43,** 251.
Popp (R. K.) and Gilbert (M. C.), 1972. *Am. Mineral.* **57,** 1210.
Råheim (A.) and Green (D. H.), 1974. *Contrib. Mineral. Petrol.* **48,** 179.
Schliested (M.), 1978. Ibid. **66,** 105.

[*Manuscript received 10 September 1979; revised 29 October 1979*]

COMPOSITIONAL ZONING IN THE BLUESCHIST FACIES SODIC AMPHIBOLES

Robert Muir Wood
Department of Mineralogy and Petrology,
Cambridge.

Appendix 1.

The method utilised here in order to calculate the ferrous and ferric iron content of the amphibole unit cell is the, by now familiar, solution of the two simultaneous equations that are considered inherent within the nature of the crystal structure: charge balance and site occupancy. The method can be justified only if the total number of unknowns for the crystal chemistry is strictly limited. For minerals such as stilpnomelane in which the ferrous/ferric iron ratio is directly related to the hydroxyl content (and thus the charge balance) the interdependence within the second equation obstructs ferrous/ferric iron calculation. The amphiboles, although potentially suitable for the method, require rationalisation.

Site occupancy equations are valid only if there are no vacancies within the normal structural sites. Although Neumann (1976) showed that high pressure minerals have full site occupancy, within the amphibole structure there is an excess site (the 'A' site) that is vacant at low temperatures and becomes filled by an alkali atom within hornblendes etc. Yet whilst the total number of cations may vary between 15 - 16 it is possible to avoid the criticisms of Misch and Rice (1975) concerning the effect of this variability upon recalculation of ferrous and ferric iron by disjunctive alternatives: either 1) if the sum of potassium, sodium and calcium ions is less than two within the unit cell formula, then the recalculation is performed with a cation sum of 15; or 2) if the sum of potassium, sodium and calcium within the unit cell formula is greater than two then the recalculation is performed for a 13 cation unit cell for which the Na+Ca+K content is ignored. The major assumption required for this procedure is that the larger calcium, sodium and potassium ions can never be located on the smaller M_1,M_2 and M_3 sites. The subsidiary assumption is that when the 'A' site is to some degree filled, the smaller divalent cations do not bleed over into the M_4 site. Such ambiguities are particularly significant for high manganese contents. The first, and most important assumption can, however, be validated by wet chemically determined analyses and in fig. 1, two histograms have been constructed to display the variations away from these ideals within blueschist amphiboles taken from the published analyses of Ernst et al. (1970), Onuki and Ernst (1969), Makanjuola and Howie (1972) and Bocquet (1974). Those taken from the work of Bocquet have average total cation contents of 14.999(!); the standard deviation for all these analyses for summing to '15' is 0.11; and for summing to '13', neglecting the alkalies and calcium, is only 0.06.

As a form of error manipulation those that lie outside the limit of 0.05 to either side of the predicted value have been replotted for the alternative cation sum and are displayed as internal black histograms, also in fig. 1. Although the standard deviation of these replotted compositions is greater than that of the overall distribution, the re-allocation of '15' to '13' and '13' to '15' clearly improves accuracy; some of the larger 'double errors' may be from poor quality wet chemical analysis.

Any error within this assumption of full and discrete cation site occupancy becomes magnified within the recalculation of ferrous/ferric iron content. The difference between the true cation sum and the assumed cation sum becomes multiplied by 46/15 for summing to '15' and 46/13 for summing to '13'. The resultant error in ferrous/ferric iron relative concentrations may be highly significant, particularly for low total iron contents. Whilst the statistical analysis of wet chemically determined analyses vindicates the assumptions of full cation occupancy, it can only emphasise that individual analyses may be of low accuracy, that is compounded by errors within the microprobe analysis. Such errors should not, however, produce any *overall* bias. Only a statistical analysis of a large number of microprobe and wet-chemical analyses of exactly the same unzoned, uncontaminated amphiboles could finally prove the method.

The second equation necessary for the recalculation of ferrous/ferric iron content assumes a constant anion charge balance. Unfortunately this also is a poorly defined constant; Leake (1968) showed that there may be between 1 and 3 hydroxyl groups within the amphibole structure in place of the ideal 2. Whilst the limits of a 'good' amphibole analysis have remained controversial, authors who have considered the determinative procedure for ascertaining water content suspect, have taken to recalculating even wet-chemical analyses on an anhydrous basis of 23 oxygens (Miyashiro,1957; Makanjuola and Howie, 1972). Thus the 23 oxygen anion content assumed here is taken as one of convention if not of empirical truth.

References

Bocquet (J.),1974. Schweiz.Mineral.Petrog.Mitt.,54,425.

Ernst (W.G.), Seki (Y.), Onuki (H.) and Gilbert (M.C.),1970. Geol.Soc.Am.Mem.,124,1.

Leake (B.E.),1968.Geol.Soc.Am.Spec.Paper,98,1.

Makanjuola (A.A.) and Howie (R.A.),1972.Contrib.Mineral. Petrol.,35,83.

Misch (P.) and Rice (J.M.),1975.J.Petrol.,16,1.

Miyashiro (A.),1957.J.Fac.Sci.Univ.Tokyo,11,11,57.

Neumann (E-R.),1976.Norsk.Geol.Tiddskrift,56,1.

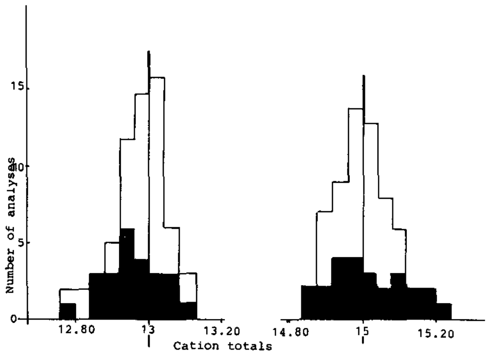

fig. 1. Amphibole site occupancies within wet-chemically determined analyses recalculated both with and without the (Na+Ca+K) content.